Hydrokinetic energy conversion: Technology, research, and outlook

Nicholas D. Laws, Brenden P. Epps *

Thayer School of Engineering, Dartmouth College, 14 Engineering Dr., Hanover, NH, USA

ARTICLE INFO

ABSTRACT

Interest in the advancement of *hydrokinetic energy conversion* (HEC) technology has grown substantially in recent years. The hydrokinetic industry has advanced beyond the initial testing phase and will soon install demonstration projects with arrays of full-scale devices. By reviewing the current state of the industry and the cutting edge research this paper identifies the key advancements required for HEC technology to become commercially successful at the utility scale. The primary hurdles are: (i) reducing the cost of energy, (ii) optimizing individual turbines to work in concert considering array and bathymetry effects, (iii) balancing energy extraction with environmental impact, and (iv) addressing socio-economic concerns.

This review is split into three primary sections. The first section provides an overview of the HEC technology systems that are most likely to be installed in commercial arrays. The second section is an in-depth literature review. The literature review is sub-divided into five areas that are positioned to significantly impact the viability of HEC technology: (i) site assessment, (ii) turbine design, (iii) turbine wake modeling, (iv) array performance, and (ν) environmental impact. The final section presents an outlook for the HEC industry and future research.

Contents

---

* Corresponding author. Tel.: +1 603 646 6656.
  E-mail address: bepps@dartmouth.edu (B.P. Epps).

1. Introduction

With the growing recognition of global warming, more governments, research centers, and corporations are committing resources to the advancement of renewable energy technologies. There is not one renewable energy resource that will be a panacea for the world's energy needs. In order to transition from fossil fuel based energy resources, humankind must tap into a variety of renewable resources. As each country evaluates its resources, many have recognized hydrokinetic energy as a significant contributor to its renewable energy portfolio.

The purpose of this review is to summarize and synthesize the most crucial areas of research necessary to advance *hydrokinetic energy conversion* (HEC) technology towards widespread commercialization. In doing so, another aim of this review is to place a stake in the ground from which more advanced, cross-disciplinary work may be launched. HEC research encompasses a wide range of fields, including materials, fluid mechanics, and marine-biology (just to name a few). Furthermore, social and economic factors present significant hurdles to future HEC installations. This review touches on all of these areas and more.

The review begins with a summary of the most-advanced HEC technologies. It then takes the point-of-view of a design engineer by reviewing the cutting-edge research across all steps of project development. HEC research and development is a rapidly changing field and researchers are working to address numerous open questions. Questions range across all steps of project development: from site assessment, such as how to best characterize the resource at a site of interest; to device design, such as how to predict unsteady rotor loads and fatigue; to long-term operation, for example understanding the environmental impact of a large array of hydrokinetic turbines.

Finally, the review closes with an outlook for the HEC industry. A summary of the most advanced HEC projects across the globe is presented along with the non-technical hurdles that current HEC projects are facing. The review closes with a summary of the key hurdles identified and the steps that must be taken to address them.

2. Technology

Hydrokinetic energy converters can tap into three types of resources: *inland* (rivers), *tidal* (estuaries and channels), and *ocean* (currents). Most of the research and development of HEC technology to date has been directed towards tidal systems, and there has been relatively little development for inland or ocean current devices. Inland sites generally face more user conflicts than tidal or ocean sites. Ocean current device developers face a major hurdle in designing economical mooring systems for deep water sites [151].

Until recently, the HEC industry was dominated by small, entrepreneurial companies. In the last three years, however, a handful of large engineering and manufacturing firms have entered the field, primarily by buying designs near commercialization. The most active countries include the United Kingdom,

Ireland, France, Spain, China, Japan, South Korea, Canada, and the United States [79]. Europe is at the forefront of technology development, with much of the activity in the UK due to its abundant wave and tidal resources. The European Marine Energy Center (Orkney, Scotland) provides plug-and-play testing sites and is currently developing international standards for the tidal and wave power industries [47].

In the following subsections, the most advanced designs in industry are presented. The subsections are defined by the three primary configurations of HEC systems: *axial-flow*, *cross-flow*, and *oscillating*. There are many designs that are in the conceptual and scale-model stages that are not mentioned in this review. Lago et al. [89] gives a comprehensive overview of the wide range of concepts for HEC systems. Here, the focus is on the systems that are closest to commercial-scale production.

2.1. Axial-flow systems

The vast majority of HEC systems are lift-based, axial-flow, tidal turbines. Drag-based systems do exist but they suffer from lower efficiencies compared to lift-based systems [6,73]. However, drag-based HEC systems can be useful in extracting energy from flows with exceptional amounts of debris, which is an important consideration for some sites [71].

Lift-based, axial-flow turbines use the same principles as aircraft wings, propellers, and wind turbines. The blades of a lift-based turbine are composed of two-dimensional hydrofoil cross-sections. Fig. 1 illustrates the velocities and forces (per unit radius) on a blade section: axial inflow velocity V_a and angular velocity ω. The effective freestream has magnitude $\sqrt{V_a + \omega r}$ and is oriented at pitch angle β to the rotor plane. The blade is pitched by angle θ such that a favorable angle of attack α is achieved, resulting in a lift force as shown. The lift and drag combine to produce torque $Q = (L \sin \beta - D \cos \beta)r$. The power extraction is then $Q\omega$. This shaft power is converted to electricity by a generator either directly coupled to the shaft (perhaps via a gearbox) or indirectly coupled via hydraulic transmission [18,122].

The lift force is the net resultant of the fluid pressure acting over the hydrofoil surface. Fig. 1 illustrates the pressure distribution for the exemplar case of a NACA 4418 hydrofoil at 4° angle of attack. Computations were performed using open-source code XFOIL [34], which employs a potential flow panel method coupled with an integral boundary layer solver. Because of the asymmetric (top-to-bottom) hydrofoil shape, water flows faster over the upper surface than the
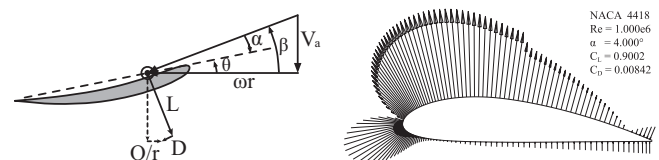

Fig. 1. (Left) Axial-flow turbine blade cross-section velocity and force triangles. (Right) Pressure distribution over a NACA 4418 hydrofoil at 4° angle of attack, computed using XFOIL [34].
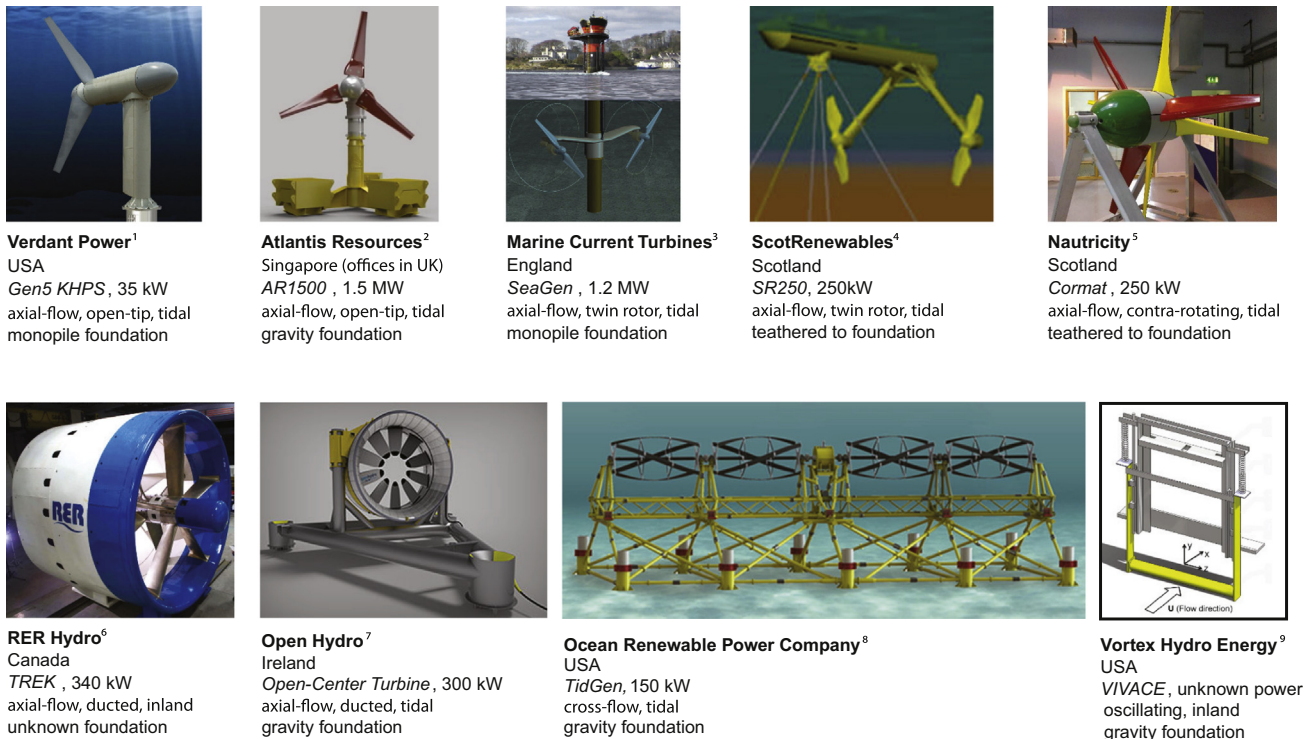
Verdant Power[1]
USA
Gen5 KHPS , 35 kW
axial-flow, open-tip, tidal
monopile foundation

Atlantis Resources[2]
Singapore (offices in UK)
AR1500 , 1.5 MW
axial-flow, open-tip, tidal
gravity foundation

Marine Current Turbines[3]
England
SeaGen , 1.2 MW
axial-flow, twin rotor, tidal
monopile foundation

ScotRenewables[4]
Scotland
SR250, 250kW
axial-flow, twin rotor, tidal
teathered to foundation

Nauticity[5]
Scotland
Cormat , 250 kW
axial-flow, contra-rotating, tidal
teathered to foundation

RER Hydro[6]
Canada
TREK , 340 kW
axial-flow, ducted, inland
unknown foundation

Open Hydro[7]
Ireland
Open-Center Turbine , 300 kW
axial-flow, ducted, tidal
gravity foundation

Ocean Renewable Power Company[8]
USA
TidGen, 150 kW
cross-flow, tidal
gravity foundation

Vortex Hydro Energy[9]
USA
VIVACE , unknown power
oscillating, inland
gravity foundation

Fig. 2. Advanced industry designs. Image references: [1][158], [2][7], [3][99], [4][136], [5][107], [6][126], [7][120], [8][119], and [9][23].

lower surface. By Bernoulli's principle, this fast flow is associated with low pressure, resulting in a suction as shown.

The current leading designs for lift-based, axial-flow, tidal turbines are summarized in Fig. 2. Also of note, but not pictured, are the designs by Andritz Hammerfest (Norway), Voith Hydro (Germany) and Alstom Power (France). Each of these are three-bladed, axial-flow systems; the Voith and Alstom designs use monopile foundations similar to Verdant Power, whereas Andritz uses a gravity base similar to Atlantis.

Verdant Power (see Fig. 2) is the most active US axial-flow company. From 2006 to 2009 Verdant tested six full-scale prototypes in the East River in New York City, making it the first commercially-licensed array of tidal turbines in the world [158]. The Verdant design uses a passive yaw system to align the with the flow. Most recently, Verdant has partnered with the University of Minnesota to study turbine array spacing and with the Oak Ridge National Laboratory to study fish–turbine interactions [158].

The marine current turbines *SeaGen* design (see Fig. 2) was the world's first commercial-scale tidal generator [99]. The SeaGen is unique due to its horizontal support arm, which can be raised and lowered to allow service of the turbines above the water surface. This design is limited to shallow tidal sites, with depths limited by the practical height of the tower. Siemens purchased marine current turbines in 2012 and has a handful of sites under development in the UK, but more recently Siemens announced that it will sell marine current turbines due to slow development in the industry [100,64].

The Scotrenewables *SR250* turbine (see Fig. 2) is remarkable due to its unique transport and survival mode. The twin turbine support arms fold up to parallel the long, slender platform for towing the floating system or to protect the turbine during storm events. Scotrenewables is currently developing a 2 MW version of their proven 250 kW prototype [136]. Buoyant systems have a great advantage over bed mounted systems in that the installation and maintenance costs of buoyant systems are significantly less.

The Nauticity *Cormat* design (see Fig. 2) has two rows of contra-rotating blades and is moored by a single point at the front of the floating turbine [25]. In this fashion, the turbine can align to the flow stream passively. The Cormat is currently in commercial-scale testing.

The OpenHydro *open-center turbine* design (see Fig. 2) places the generator along the circumference, thus eliminating a central shaft and shaft seals [143]. Through an agreement with the Public Utility District of Snohomish County, OpenHydro plans to install two 300 kW turbines near Seattle, Washington [2]. OpenHydro also has projects developing in Europe and Canada [120].

The RER Hydro *TREK* (Kinetic Energy Recovery Turbine) (see Fig. 2) is a ducted, multi-stage turbine that has three rows of blades, with the first and last rows acting as stators [126]. The TREK has been in full-scale testing since 2010. In 2012, RER Hydro partnered with Boeing, giving Boeing the rights to sell and market the RER hydro technology [16].

One final interesting design of note is the Flumill by the company of the same name in Norway [48]. The Flumill consists of large, buoyant, bed-mounted, and twin Archimedes screws. The Flumill is currently undergoing commercial-scale testing [48].

2.2. Cross-flow systems

Cross-flow turbines rely on the same principles as lift-based axial flow turbines to develop a pressure differential across blade-sections. However, cross-flow systems orient the axis of rotation normal to the freestream (versus parallel to the freestream for axial-flow systems). Therefore, as a cross-flow turbine rotates the angle of attack of each blade varies cyclically. The cyclical variation of the angle of attack creates cyclical blade loading, which increases the fatigue experienced by blades. Much of the cyclical loading can be alleviated by using helical instead of straight blades. Helical cross-flow turbines are also known as Gorlov turbines (see Fig. 3).
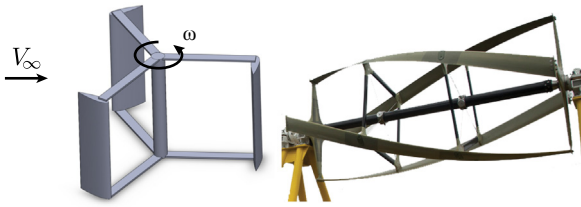
Fig. 3. Examples of a straight-bladed [57] and helical-bladed cross-flow turbine [119].
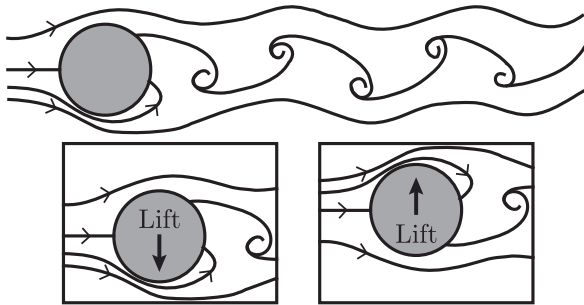

Fig. 4. Illustration of von Kármán street in the wake of a cylinder and the induced vibrations. Inspired by [87].

Though cross-flow turbines are generally less efficient than axial-flow turbines, they do have some distinct advantages: cross-flow turbines can have a rectangular cross section, which allows them to be more efficiently packed in arrays than circular-cross-section axial-flow turbines. Another benefit is the ability to generate power from any flow direction that is perpendicular to the axis, which is extremely advantageous in a tidal flow [9].

Many small cross-flow systems are available commercially; however, only one design is positioned to make a significant impact on renewable energy production. Ocean Renewable Power Company (ORPC) is the most active cross-flow turbine producer in the US. ORPC has developed and tested tidal and inland systems. They also have designed an ocean current system. ORPC has tested their tidal turbine (see Fig. 2) off the coast of Maine in a partnership with the University of Maine [121] and has tested their inland turbine in Alaska through a partnership with the University of Alaska [4]. ORPC currently has a preliminary permit for the Cook Inlet in Alaska for site research until 2016 for up to 100 MW of installed capacity.

2.3. Oscillating systems

Oscillating systems using flapping foils [149,76] have been proposed, but they suffer from a complex control system, which is necessary to maintain the wing's optimal angle of attack to create enough lift for power production. The control system is also required to overcome the pitching moment of the wing and reverse the direction of oscillation.

The most successful oscillating system to date uses vortex induced vibrations to generate energy. Vortex induced vibrations occur due to the periodic shedding of vortices in the wake of a bluff body. The visual presentation of this phenomenon is known as a *von Kármán street*, which is illustrated in Fig. 4. The periodic vortex shedding is associated with alternating low-pressure regions on the upper and lower sides of a cylinder, resulting in an unsteady periodic lift force. The non-dimensional vortex shedding frequency (Strouhal number) for a cylinder is roughly constant $St = fd/V \approx 0.2$ over a wide range of flow speeds V and cylinder diameters d. In a high-Reynolds-number turbulent flow,

the wake is not clean as illustrated in Fig. 4, but the lift force still exhibits statistical fluctuations corresponding to $St \approx 0.2$ [87]. By designing the system to resonate at this desired frequency and equipping the system with power take-off elements, vibrational energy harvesting is achieved.

There appears to be only one oscillating system nearing commercial production. The VIVACE (vortex induced vibrations for aquatic clean energy) system, designed at the University of Michigan (see Fig. 2), makes use of vortex induced vibrations to drive cylinders transverse to the flow, with a linear generator providing the power take-off. These devices are designed to be placed inline with each other in close proximity, which allows for dense array spacing [15]. Another advantage of the VIVACE design is the ability to extract energy from flows as slow as 0.4 m/s [23]. The VIVACE group is currently performing full-scale testing. No other oscillating design is as mature as the VIVACE system.

3. Research

This section reviews the cutting edge research regarding HEC technology. The outline of this section follows a simplified design path, shown graphically in Fig. 5. Note that two-way arrows connect each area. These connections represent the dependence of each area of research on the others, and the true picture is much more complex with arrows going between each area, not just around the design loop shown here. For example, a hydrokinetic device should really be designed not just with the site parameters in mind, but also how it will perform in an array of devices. Also note that the *site* and *environment* are one and the same, but they are shown separately here to reflect the organization of this paper (Fig. 5).

The design process begins with a given site. Site characteristics act as inputs to all stages of development, from initial system design to decommissioning of an array of turbines. The issues regarding site assessment are covered in Section 3.1. Once a site has been characterized, turbine design can begin. In Section 3.2, research regarding turbine design in terms of performance, reliability, and economics is reviewed. In arrays, turbines interact with one another primarily through their wakes. Turbine wake modeling research is discussed in Section 3.3. Turbine array modeling and optimization is then reviewed in Section 3.4. Finally, once an array design is optimized, there remains one major hurdle to a HEC project: environmental impacts. The environmental impacts of large turbine arrays are still unknown, as discussed in Section 3.5. In order to gain public support for HEC technology, researchers must identify high potential sites, design
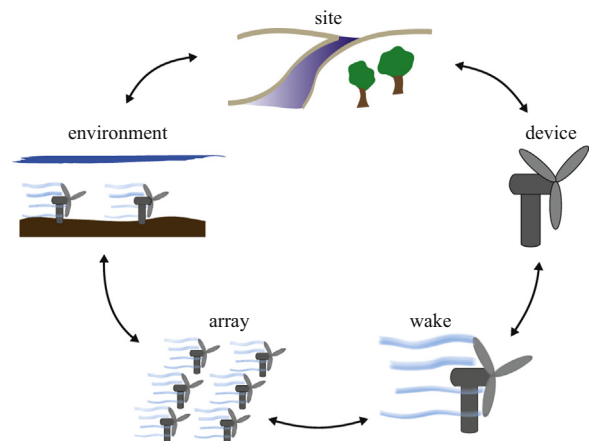

Fig. 5. Summary of design considerations for hydrokinetic energy conversion systems.
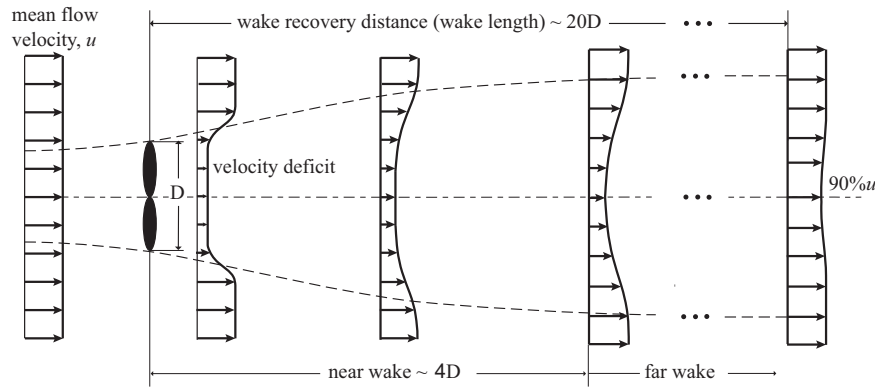
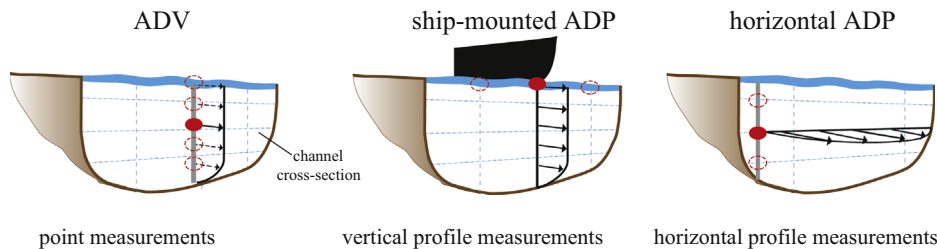**Fig. 6.** Definition of wake characteristics. Figure adapted from [11].

Fig. 7. Flow characterization using acoustic Doppler instruments. Figure adapted from [108].

robust and cost-effective turbines that operate efficiently in arrays, and demonstrate that any environmental detriment of these arrays is outweighed by the environmental gains realized from producing renewable energy (Fig. 6).

3.1. Site assessment

Attempts have been made on a broad scale to estimate the resource of available hydrokinetic energy. Unfortunately, these large scale estimates have a significant degree of error. For example, the US tidal estimate model was found to differ from some actual, spot-checked site flow velocities by 30% or more, which can lead to an error of a factor of two or more in the total estimate [98]. Furthermore, global tidal potential estimates range from 100 TWh/yr up to 17,500 TWh/yr, which represents a difference of two orders of magnitude [143]. These examples highlight the importance of specific site assessments in determining the hydrokinetic resource for a given project.

There are three types of resource estimates [98]:

- *theoretical resource*: total average annual hydrokinetic energy available;
- *technical resource*: energy that can be extracted by present HEC technology; and
- *practical resource*: energy that can be extracted considering all practical factors [present HEC technology, debris mitigation (e.g. logs and sediment), user conflicts (e.g. maintaining shipping routes), etc.].

Resource estimates for the US are summarized in Table 1. For context, US electricity consumption is roughly 4000 TWh/yr [150]. Therefore, the total theoretical resource estimate including inland, tidal, and ocean is slightly more than 90% of US electricity consumption. More than 50% of the US tidal resource is located in Alaska [5]. Note that the practical resource has not been estimated, although it is the most valid when considering the viability of a hydrokinetic project. Determining the practical

Table 1

Hydrokinetic resource estimates for the United States. Ocean resources include a portion of the Gulf Stream within 200 miles of the coast.

	Inland	Tidal	Ocean
Theoretical resource	1433 TWh/yr[a]	445 TWh/yr[b]	163 TWh/yr[d]
Technical resource	120 TWh/yr[a]	250 TWh/yr[c]	n/a

[a] Ref. [37].
[b] Ref. [55]
[c] Ref. [35].
[d] Ref. [56].

resource requires a detailed site assessment and consideration of all exogenous factors affecting an installation.

3.1.1. Detailed flow characteristics

Accurately determining the detailed flow characteristics of a site is critical for determining the technical resource and the magnitude of the loads that structures placed in the site will experience. The best practices for assessing the flow characteristics of a hydrokinetic site are outlined in [108], though it should be noted that best practices are still evolving [58].

Acoustic Doppler instruments are important and widely used tools in site assessments (as well as experimental studies [109,11]). With acoustic Doppler instruments, researchers can determine a site's velocity field, turbulence intensity, and power density [58]. Accurate measurements of these parameters are crucial for identifying the most power dense locations within a site, determining spatial and temporal variations in the resource, and estimating the loads that devices will experience once installed. For a discussion of the errors associated with Doppler instruments see [127].

There are two main types of acoustic Doppler instruments (see Fig. 7) : *acoustic Doppler velocimeters* (ADV), which yield point measurements and *acoustic Doppler profilers* (ADP), which yield a set of simultaneous measurements along a line. ADVs have higher spatial and temporal resolutions than ADPs, so ADVs are preferred for turbulence studies. However, ADPs are less expensive operationally and are therefore preferred for wide-scale or long-term

site assessments. Researchers are investigating the use of more economical ADP tools for turbulence measurements and ways to reduce the costs of ADV studies [58].

Gunawan et al. [58] deployed ADVs for two months at the hub height of a specific turbine design. Taking a page from the wind power industry, Gunawan et al. [58] proposes that the hydrokinetic industry defines a standard classification system for tidal sites to allow comparison between potential sites and to determine which type of turbine is best suited for any given site.

Polagye and Thomson [123] outline a methodology to analyze the data collected from ADPs. They report that deploying ADPs for a minimum of 30 days with a 1 Hz sampling frequency is sufficient to predict device performance. However, pointing to the fact that a number of tidal turbines have failed due to the underestimation of design loads, they estimate that a year of data collection is necessary to accurately predict the peak loads that a device will experience during its lifetime.

3.1.2. Wave spectrum characterization

Waves have not been a focus of site assessments in the past. Historically, HEC sites have been intentionally located in sheltered areas with devices far enough from the surface to make the effects of waves a secondary consideration [108]. However, as more energetic sites are developed it is anticipated that wave–turbine interactions will become a factor. The wave power industry is developing techniques for the characterization of wave spectrums, and these techniques are anticipated to carry over to the hydrokinetic industry.

3.1.3. Bathymetry and bed surface characteristics

Determining the bathymetry of a site is key to micro-siting turbines within a site (discussed further in Section 3.4). The make-up of the bed surface can determine the type of mooring to be employed, as well as possible soiling issues that devices could face. To map a site's bathymetry, the common practice is to employ GPS tools coupled with ship-mounted depth echosounders [108]. Bed surface characteristics are typically determined through direct sampling. Loose sediments are collected with ponar-type grab samplers, and core samples are used to examine the underlying bed material [108].

3.1.4. Site access

Most of the site access research has been for offshore applications, where the two primary concerns are proximity of a port and the availability of specialized ships to install and retrieve HEC systems. Researchers and leading manufacturers have concluded that the most cost-effective method of accessing offshore turbines is to own and operate a custom-designed ship [14]. Maisondieu et al. [97] give an overview the types of ships available for the various tasks associated with offshore sites; they also discuss the best practices for installation procedures to minimize costs.

Inclement weather also factors into site access, since waiting for the right weather can increase the cost of a hydrokinetic project because ships must be held and paid for during wait times [139]. Historical data for wave height, current speed, and wind speed allow developers to predict the accessibility of a site and determine the best times of year for installation and maintenance tasks [140].

3.2. Turbine design (performance, reliability and economics)

After determining the design parameters from a site assessment, turbine design is the next step in a design process. Performance and reliability of hydrokinetic turbines are of primary research interest, and both are tied directly to the economics of the overall device design. For HEC technology to compete with traditional energy

sources it must be shown that HEC systems can reliably produce a significant amount of energy at reasonable costs.

The key issues regarding HEC system design are as follows:

- Hydrodynamic rotor design (i.e. conversion of hydrokinetic power to shaft power):
  ○ Hydrofoil and blade design.
  ○ Hydro-elastic load coupling.
  ○ Yaw and wave effects.
- Power take-off system design (i.e. conversion of shaft power to electrical power).
- Structure and mooring system design.
- Economics and engineering trade-offs:
  ○ Balancing performance, reliability, and cost trade-offs.
  ○ Balancing performance and structural trade-offs.
  ○ Predictive maintenance.
  ○ Economic comparison across types of HEC systems.

In order to contain the scope of this paper, a thorough review of only some of these points is covered in the following sections.

3.2.1. Hydrofoil and blade design

Hydrokinetic energy extraction begins where moving water meets turbine blades. Turbine blades are made up of hydrofoil section profiles, varying from hub to tip. Shiu et al. [138] have designed a family of hydrofoils for marine hydrokinetic devices: Their designs are based on airfoils that are optimized for low vulnerability to cavitation and singing, low susceptibility to fouling, and high performance in the usual airfoil characteristics (lift-to-drag ratio, stall behavior, etc.).

Blade design is facilitated by engineering codes, typically based on *blade element momentum theory* or *rotor lifting line theory*. HARP_Opt [132] and OpenProp [38,39] are representative open-source engineering codes for preliminary design of axial-flow turbines. (OpenProp is also useful for marine propeller design, hence its name.) HARP_Opt employs blade element momentum theory and uses a multi-objective genetic algorithm to maximize annual energy production subject to constraints such as cavitation. OpenProp employs rotor lifting line theory [43] and principles from variational calculus to optimize the blade load distribution (lift coefficient) for maximum power extraction, with options for blade geometry (chord and thickness) optimization subject to cavitation and stress constraints [42]. OpenProp also provides performance curves for off-design flow conditions, blade cavitation and stress analyses, and geometry outputs for visualization and modeling [40].

Engineering models have also been developed for crossflow turbines, such as CACTUS [101] and CyROD [41]. The CyROD model accounts for six load effects: steady lift, steady drag, lift due to flow curvature, unsteady lift, added mass, and acceleration reaction [129,130]. Both models employ a vortex-lattice formulation with a free-wake model, with shed vorticity advected with the freestream plus the induced velocity field for more accurate performance predictions.

Leading-edge slats have been shown to significantly increase a hydrokinetic turbine's performance [163]. By introducing more energized flow to the leading edge of a hydrofoil, slats increase a hydrofoil's lift coefficient, lift-to-drag ratio, and stall angle. This leads to an increased power coefficient for turbines employing leading-edge slats.

Bidirectional hydrofoils can eliminate the need for pitch control mechanisms in tidal systems, which can sometimes be used to prevent cavitation. Nedyalkov and Wosnik [111] experimentally evaluated the cavitation performance of a bidirectional NACA hydrofoil and compared it to its unidirectional counterpart. They found that, compared to the unidirectional profile, the bidirectional profile has

similar lift properties, slightly higher drag, and better cavitation performance. Their finding is promising for tidal devices because, by eliminating pitch control mechanisms, the capital and maintenance costs of a tidal system are reduced.

Blade soiling and fouling is another concern regarding the performance and reliability of hydrokinetic turbines. The addition of weight to turbine rotors in the form of soil and other adherent substances can lead to increased loads and decreased performance. Walker et al. [159] investigated artificial fouling on a two-bladed axial-flow turbine model. They compared the turbine's performance using three different cases: baseline clean blades, blades soiled with grease and abrasive powder to represent biological slime fouling, and blades roughened with contact cement to represent hard biological fouling such as barnacles. The artificially slimed blade actually exhibited improved performance; most of the grease and powder sloughed off of the blade and what was left was found to delay stall. However, the blades roughened with contact cement were found to have a 19% reduction in the maximum power coefficient (from 0.42 to 0.34) compared to the baseline clean blades.

3.2.2. Hydroelastic models

Since arrays of turbines will be installed in highly-energetic flows, turbines will be subjected to large and variable turbulent forces [50]. This has prompted researchers to develop hydroelastic numerical models to investigate the coupled effects of hydrodynamic loads on the elastic structures and the performance of HEC devices.

The hydroelastic design of a turbine rotor amounts to multi-objective design optimization with the goals of simultaneously maximizing the power coefficient and minimizing the blade stress. Kolekar and Banerjee [86] perform this optimization via a genetic algorithm, using *blade element momentum theory* and *Euler–Bernoulli beam theory* for the hydrodynamic and structural models, respectively. Their analysis compares the hydroelastic performance of a constant-chord straight blade to a variable-chord twisted blade; after optimizing both blade designs, they found that the twisted variable-chord blade had a 17% higher power coefficient. This increase in performance comes at the cost of manufacturing more complex blades.

An open-source code, `Co-Blade` [133], was developed to optimize composite blades for axial-flow wind and hydrokinetic turbines. This model combines *classical lamination theory* with *Euler–Bernoulli beam theory* and *shear flow theory* to create a simplified model that allows for parametric design optimization. Sale et al. [133] perform a Monte-Carlo analysis on various composite blade properties to determine those that have the greatest and least impacts on the strength of the blade and identifies some pathways to reduce the costs of blades and increase their reliability, such as removing excess material.

Composite blade design have also been considered for cross-flow turbines [90]. Due to the unsteady flow field induced by cross-flow turbines, Li et al. [90] used a *discrete vortex method* with *finite element analysis* for the hydroelastic model. They found that both failure probability and power coefficient increase with the height-to-radius ratio of a three-bladed vertical-axis cross-flow turbine. For the particular turbine studied, the structural limit of the blades was reached at a height-to-radius ratio of three. Therefore, while increasing height-to-radius ratio improves hydrodynamic performance, a practical limit is reached due to structural limitations.

3.2.3. Yaw and wave effects

Passive or active yaw systems can increase rotor performance and reduce the unsteady loads on turbine blades [50]. For example, data from one multi-year site assessment show that a passive

yaw system could yield a 5% improvement in energy extraction over a turbine without a yaw system [123]. Of course, this possible improvement depends on the variability in flow direction at the site. Therefore, for some sites the performance and structural gains might be outweighed by the increased maintenance and capital costs that come with adding a yaw system.

The influence of waves (on turbine performance and loading) has only recently become an area of focus. Limited experiments thus far (with a two-bladed axial-flow turbine) show that the time-averaged power and thrust coefficients are independent of wave height, but the instantaneous thrust, rotational speed, and torque vary significantly with each wave passage [93,91]. Galloway et al. [50] are developing a blade element momentum model for axial-flow turbines, which accounts for both yaw and wave effects. They are also conducting laboratory experiments to investigate these same effects and confirm their numerical model. They found that wave frequency has a larger effect than wave amplitude on maximum blade loads, similar to the findings of [93] and [91].

3.2.4. Predictive maintenance

Predictive maintenance systems monitor the health of a device and use the data collected to either inform operators of a maintenance need or to alter a device's operation mode to minimize maintenance requirements. Predictive maintenance is a nascent research area [121], and it will play an important role in decreasing the operation and maintenance costs of HEC systems. A first step in developing predictive maintenance systems is designing sensors for monitoring a turbine's health *in situ*. Schuster et al. [135] evaluated the effectiveness of bonding fiber optic strain sensors to the exterior of composite turbine blades; they found that the sensors did not stand up to simulated operating conditions, and they recommend that the sensors be embedded in the blade structures to protect them from the harsh marine environment.

3.2.5. Economic comparison across types of HEC systems

The US Department of Energy (DoE) has defined a *levelized cost of energy* (LCOE) calculation method to allow comparisons across HEC technologies [88]. LCOE estimates are given for the DoE Reference Models for arrays of 10 and 100 units by [110]. The ocean current model is found to be the most economical at 25 cents/kW h for a 10 unit array, due to the high capacity factor that comes with a consistent ocean current and the ability to scale up to larger capacities (since there are no physical site constraints in the open ocean). Next is the tidal turbine model at 41 cents/kW h for a 10 unit array, slightly more than US offshore wind cost predictions. The inland model is estimated at 80 cents/kW h for a 10 unit array. Their estimates indicate that (in all three cases) capital expenses are likely to greatly outweigh operating expenses for HEC projects. Among the capital expenses, the structural and energy conversion components are found to be the key cost drivers.

A more recent LCOE analysis by Jenne et al. [70] estimates costs for a 10 MW commercial-scale installation for the three resource types: The ocean current array is estimated to cost 48 cents/kWh (3 devices), the tidal array 42 cents/kWh (9 devices), and the river array 31 cents/kWh (111 devices). This price trend is opposite that of Neary et al. [110], since Jenne et al. [70] hold the total power fixed at 10 MW whereas Neary et al. [110] hold the total number of devices fixed at 10. Since the devices have different rated powers, a different number of devices is needed for each scenario, leading to differences in economy of scale.

To perform a cost comparison between wind and tidal technology capital costs, an economic analysis for the DoE reference tidal turbine [110] was performed using off-the-shelf components from the wind industry [14]. To calculate a tidal system's capital

cost, additional costs relative to wind systems must be taken into account, including redundant subsystems to increase maintenance intervals, additional seals, and higher gear box cost (for lower shaft rpm). Beam et al. [14] estimate the total capital cost for a 500 kW tidal turbine to be $1150/kW with redundant systems and $950/kW without redundant systems; for comparison, the cost of a 500 kW wind turbine is estimated at $700/kW.

3.3. Turbine wake modeling

Characterization of the turbine wake is crucial to understanding the effects that turbines have on each other and the surrounding environment. Modeling a turbine wake accurately can aid in determining array power extraction, as well as environmental impacts such as scour and sediment transport.

The wake region downstream of a turbine is typically characterized by four parameters: *wake width, wake length, mean velocity profile,* and *turbulence intensity.* The wake length (*recovery distance*) is the distance from the rotor plane to the point downstream where the velocity has nearly recovered to the upstream value. In addition to these geometric parameters, the wake is typically characterized by a *velocity recovery ratio* and *turbulence intensity recovery ratio*, which are typically reported at hub-height or turbine center-line.

Wake recovery is a key factor in determining the stream-wise spacing of turbines in arrays. Wake recovery is primarily driven by the mixing of the wake with the surrounding flow, which can be encouraged by higher ambient turbulence intensity [96] or by close spacing between adjacent wakes or between the wake and a boundary [142].

Turbine wakes can be divided into two regions based on idealized velocity profiles. The *near wake* is idealized as a uniform velocity deficit, with a shear layer separating the wake and free-stream. Progressing downstream from the rotor plane, the wake expands, turbulence dissipates, and the circumferential (swirl) velocity slows. The transition from *near wake* to *far wake* is defined as the point where the shear layer has reached the turbine centerline. Similar to wind turbines, axial-flow hydrokinetic turbine wakes generally exhibit the transition from near to far wake approximately four diameters downstream of the rotor plane [22].

Given this foundation, key contextual points regarding wake modeling research are as follows:

- Wake characteristics: geometry; velocity deficit and recovery; turbulence intensity, recovery, and structures.
- Effect of rotor design and performance on wake characteristics.
- Effect of channel blockage (or inter-turbine spacing) on wake characteristics.
- Interactions between the wake, freestream, and bounding surfaces.
- Extrapolation of scale-model laboratory studies to the full-scale real-world environment.

In the following sections, these ideas will be reviewed within the context of each type of turbine device: axial-flow, cross-flow, and oscillating machines.

3.3.1. Axial-flow wake experimental studies

The bulk of the research regarding HEC wake modeling has been for lift-based axial-flow turbines. Thus, experimental studies are reviewed presently, and computational studies are reviewed in Section 3.3.2.

Wake recovery distance is typically defined as the distance downstream where the centerline velocity reaches 90% of the inflow velocity [59,141]. The choice of 90% is arbitrary but follows from the fact that kinetic energy scales by velocity cubed, so a downstream turbine would only have available ($0.9^3 = $) 73% of the kinetic energy of the upstream turbine; this reduction in available energy is typically deemed acceptable [104]. (For an axial-flow hydrokinetic turbine, the 90% velocity point has been experimentally found to occur 20 diameters downstream of the rotor plane.) However, Neary et al. [109] suggests that a wake velocity recovery of 80–85% is sufficient for stream-wise turbine spacing (providing the downstream turbine with just ($0.8^3 = $) 51% of the kinetic energy of the upstream turbine). Similar to other studies, Neary et al. [109] find this lower velocity recovery to occur between 10 and 15 diameters downstream. Therefore, by accepting an additional 30% decrease in the incoming kinetic energy for downstream turbines, the stream-wise spacing between turbines can be cut by as much as half. Reducing stream-wise spacing of turbines is critical to reducing the costs of turbine arrays.

In lieu of scale-model turbines, mesh disks have been used for experimental characterization of an axial-flow turbine wake [10,59,11,29]. Harrison et al. [59] and Bahaj and Myers [11] demonstrated that the far wake of a mesh disk matches well with a similarly-scaled model axial-flow turbine. Mesh disks allow researchers to use significantly smaller experimental models, therefore reducing the size of expensive test tanks and other equipment. Given that turbines in arrays are expected to be placed in the far wake of upstream turbines (to achieve greater inflow velocities for downstream turbines), it is reasonable to use mesh disks for experiments investigating far wake effects [29].

However, mesh disk models are inappropriate for investigating near wake characteristics: Tedds et al. [144] used 3D ADV experimental data for an axial-flow turbine to evaluate the accuracy of a mesh disk model [59]; their findings indicate that mesh disk models are not accurate at replicating the near wake. Furthermore, they suggest that the isotropic turbulence models prevalent in much of the CFD research should be avoided when considering the near wake.

Early researchers found that with increasing thrust coefficient, a turbine's wake velocity deficit would persist for greater downstream distances [94]. However, more recent work contradicts this finding, showing that velocity deficit is nearly independent of thrust coefficient in the far wake [103,10,143].

Wake recovery can be enhanced or diminished based on the proximity of a turbine to the bed surface or free surface. As a turbine is brought closer to a boundary, the blockage effect accelerates the flow between the turbine and boundary, thus improving wake recovery [106]. Experiments with a mesh disk show that wake recovery is fastest when the disk edge is four diameters from the boundary [105]. However, as the distance between the disk and boundary is reduced from four diameters to zero, the flow is choked on the boundary-side of the turbine, and wake recovery diminishes on the boundary side. Adding boundary roughness exaggerates this effect [103], since the additional roughness actually reduces the mass flow rate around the boundary-side of the disk. Experiments with a three-bladed, untwisted, constant chord model turbine indicate that it is also important to consider the effect of the free-surface drop that occurs downstream of a turbine on wake recovery [85].

Using 3D acoustic Doppler velocimeters (ADV), Chamorro et al. [22] measured the 3D flow velocities for two diameters upstream and fifteen diameters downstream of a bed-mounted axial-flow turbine model (modeled after a Verdant Power design). They report that the downstream persistence of large-scale turbulent structures was independent of tip speed ratio. They also observed a leapfrogging effect: the wake expansion directly behind the turbine pushed some turbulent structures into the freestream, which accelerated these structures enough to overtake slower structures in the wake as they progressed downstream. They speculate that these sorts of interactions between turbulent

structures and the freestream could explain the presence of instabilities in the far wake that lead to wake meandering. Determining the scale of wake meandering is important for determining the placement of turbines in an array, as it could require placing turbines farther apart than if no meandering were present. Based on their observations, they propose a new method for quantifying the wake recovery based on the length scale of the turbulent structures, rather than the commonly-used velocity recovery method.

In addition to effects on turbine performance, researchers are now taking into account the effects that surface waves have on turbine wake characteristics. The presence of surface waves has been found to increase the turbulence intensity in the near wake, which could decrease the wake recovery distance compared to flows with no waves [92]. However, research regarding the effects of surface waves on the far wake has found that (for two out of three cases studied) wake recovery with waves is similar to that without waves [142].

3.3.2. Axial-flow wake CFD techniques

Various *actuator disk* methods have been widely used for modeling the far wake of axial-flow tidal turbines. However, for similar turbine operating conditions (i.e. same thrust coefficient), there is little agreement among numerous actuator disk methods [13].

One standard method is to couple an actuator disk model with the Reynolds-averaged Navier–Stokes (RANS) equations. Two ways that this coupling can be achieved include representing the turbine as an axial momentum source term in the RANS equation (referred to herein as the *actuator disk model*), or by representing the turbine with both axial momentum source terms and circumferential momentum source terms, with these source strengths computed using *blade element momentum theory* (referred to herein as the *blade element model*). Batten et al. [13] compared these two models to experimental data. For predicting the wake centerline velocity deficit, the *blade element model* was found to be slightly more accurate than the *actuator disk model* (94% versus 92%). However, regarding centerline turbulence intensity, the *blade element model* was significantly more accurate (67% versus 7%). The inaccuracy of the *actuator disk model* occurs primarily in the near wake, where this model over predicts the turbulence intensity. Batten et al. [13] conclude that the blade element model is preferable over the actuator disk model for three main reasons: wake modeling is more accurate; turbine power can be estimated; and blade element models do not require empirical turbulence source terms.

One of the most advanced CFD models to date uses a large eddy simulation [74,75] to investigate the cause of the wake meandering found in the experiments of [22]. Kang et al. [75] determine that interactions between the hub vortex and tip vortex are linked to wake meandering. The hub vortex is observed to precess opposite to the turbine's rotational direction and expand outward as it travels downstream until it meets with the wake boundary at the point of meandering initiation. Perhaps coincidentally, the point of wake meandering initiation is also the same location at which the wake transitions from near to far characteristics (at approximately four diameters downstream). This near-to-far transition is due to the combination of the blade tip vortex and the rotationally-opposite hub vortex, which dissipates the flow's swirl component. They suggest that near-hub rotor design could be used to increase the stability of the hub vortex and therefore reduce the size and intensity of a turbine's wake meandering.

Kang et al. [75] also compare their high-resolution, turbine-resolving large eddy simulation (LES) model to relatively simple actuator disk and actuator line models. Both actuator models predict much smaller scale wake meandering than indicated by

both the LES model and the experimental data [22]. Unlike the disk model, the actuator line model does create a hub vortex, but it remains stable and does not precess outward. As a consequence, the actuator line model shows that wake rotation persists much further downstream than the LES model and experiments, which leads to a significant under prediction of the turbulent kinetic energy and size of the wake meandering region. Recognizing that high-resolution models such as theirs are too computationally expensive for modeling arrays, they suggest that appropriate modifications be made to actuator models to account for the influence of the hub geometry on far wake characteristics.

Both experiments and CFD modeling of the US Department of Energy *reference tidal turbine* are currently underway: Javaherchi et al. [68] have found that a 3D blade element momentum model matches the experimental characteristics of the far wake well. Also, a rotating-reference-frame CFD model has been found to represent the near wake well, except for the contribution to the wake by the hub geometry.

3.3.3. Cross-flow systems

Relatively little research has been done on the wake of cross-flow systems. Pioneering work has recently been published by Bachant and Wosnik [8,9], who investigated the near wake of cross-flow turbines. They report the Reynolds number dependence of various results including turbine performance, velocity profiles, and turbulence intensity. Overall, Reynolds independence is achieved for $Re_D \equiv UD/\nu > 1 \times 10^6$, corresponding to an average chord Reynolds number of $Re_c \equiv \lambda Uc/\nu > 2 \times 10^5$, where $\lambda \equiv$ tip speed ratio.

3.3.4. Oscillating systems

Oscillating turbines can take advantage of the turbulent energy in a turbine wake to actually *increase* the performance of downstream turbines. There are two main oscillating systems in the literature: Bernitsas [15] introduced the VIVACE system in 2008 and Kinsey et al. [81] introduced a tandem oscillating hydrofoil prototype in 2011.

One of the key findings of Bernitsas' group is that *vortex induced vibrations* (VIV) are more dependent on Reynolds number than previously believed [125]. Ding et al. [30] summarizes some of the group's work in investigating *VIV galloping* and the use of passive turbulence control to achieve matching between experimental results and a 2D unsteady RANS model. Recent experimental and computation results can be found in [31], which shows that the number of shed vortices in the wake of an oscillating cylinder per cycle increases with the freestream velocity until galloping is reached. Once the cylinder oscillations change from VIV to fully developed galloping at $Re = 100,000$ the wake vortex pattern becomes unstable.

Kinsey and Dumas [82] present results from a 2D and 3D unsteady RANS code for analyzing tandem oscillating hydrofoils and compare it to their experimental data. They also investigate the optimal spacing for their tandem oscillating prototype using a 2D unsteady RANS model and calculate the 3D losses with a similar model to use as a corrector in their 2D model [83,84]. Most recently, this research has been extended to turbulent flow conditions [80].

3.4. Array performance

Ultimately, large arrays of HEC devices must be deployed to be viable utility-scale power plants: Since typical turbine units have capacities on the order of 1 MW, utility-scale projects will include tens to hundreds of devices in densely-packed arrays. Recently, Vennell et al. [157] presented a thorough review of the trade-offs in array design for open channels. They synthesized eight key

array effects that can be summarized along the following three themes:

- Interaction between power extraction and the available hydrokinetic resource:
  - Estimating the maximum power that can be extracted from a given channel is complex, because power extraction is correlated with a reduction in flowrate and thus a reduction in power available for extraction [51].
  - This complex relationship is seen in the 1D model of [51], which is later expounded upon in [52,153]. The model amounts to the unsteady mechanical energy equation, which is presented here as a power budget:

$$\underbrace{P_{extracted}}_{\substack{(\text{power extracted} \\ \text{by turbine rotors})}} + \underbrace{P_{dissipated}}_{\substack{(\text{power dissipated} \\ \text{in turbine wakes})}} + \underbrace{(\rho g h_\ell)Q}_{\substack{(\text{power lost to} \\ \text{background friction})}} + \underbrace{\left(\frac{1}{2}\rho u_e^2\right)Q}_{\substack{(\text{power lost to} \\ \text{exhaust stream})}} + \underbrace{c\frac{d}{dt}\left(\frac{1}{2}\rho Q^2\right)}_{\substack{(\text{power required for} \\ \text{flow acceleration})}}$$
$$= \underbrace{(\rho g \zeta_0)Q}_{\substack{(\text{total power from the} \\ \text{potential energy difference})}} \qquad (3.1)$$

  where h_ℓ is the head loss due to background friction with the bed surface and turbine support structures, u_e is the velocity at the channel exit, ζ_0 is the difference in free-surface elevations between the channel inlet and exit, and we have used the typical nomenclature: fluid density ρ, gravity g, and volume flow rate $Q = u(x)A_c(x)$. The term $c\frac{d}{dt}(\frac{1}{2}\rho Q^2)$ represents the total rate of change of kinetic energy of the fluid in the channel, where $c = \int_0^L A_c(x)^{-1} dx$ accounts for the variation in cross sectional area $A_c(x)$ along the channel length L. In terms of the velocities defined in Fig. 8 and the net force that the turbines exert on the fluid, F, the extracted power is $P_{extracted} = Fu_1$, and the 'total power lost by the flow due to the turbines' is $P_{lost} = P_{extracted} + P_{dissipated} = Fu$.
  - Maximizing the power extracted by the turbines is not equivalent to maximizing the power lost from the flow, i.e. $(P_{lost})_{max} \neq (P_{extracted})_{max} + P_{dissipated}$, since $P_{dissipated}$ and the flowrate Q also depend on $P_{extracted}$ [153].
  - The kinetic energy flux of an undisturbed tidal channel can greatly over- or under-predict the actual power potential of the channel, depending on channel geometry [51].
  - The relative amount of power lost to either background friction or to the exhaust stream depends on the geometry of the channel (shallow versus deep and long versus short). The relative amount of power lost to background friction and exhaust stream versus power extracted by the array depends on the relative size of the array to the channel [51,153].
- Micro-siting of turbines within an array:
  - Turbines perform differently in arrays than they do in isolation. To achieve maximum array efficiency, individual turbines must be tuned by adjusting the flow velocity through each turbine. The optimal tuning is a function of channel geometry, array size, and individual turbine arrangements [153].
  - Due to the *blockage effect*, individual turbines within arrays can have power coefficients exceeding the *Betz limit* [52].

- Adding an additional turbine to a row may increase or decrease the power per turbine, depending on the relative size of the array to the channel [51,153,154].
- Adding an additional row of turbines decreases the power per turbine (diminishing return on investment), but overall array power output increases [155].
- Array economics:
  - Structural loads on the turbines, and thus construction costs, scale with turbine power output. Thus, higher individual turbine power output results in higher construction costs [156].

Most of the work in modeling hydrokinetic arrays has focused on optimizing the power extraction efficiency of an array of turbines operating in a tidal channel (as opposed to a river or open-ocean scenario). This is a reflection of the state of the industry and the fact that the most economically feasible sites identified to date are tidal channels.

3.4.1. Array theoretical research

Building upon the foundation of [51,52,153], recent theoretical research has extended these ideas to ocean currents and investigated intra-array turbine arrangement.

Garrett and Cummins [53] derived an analytical model for the theoretical power potential of an unbounded ocean current or tidal flow. Their analysis shows that the maximum power of a circular array depends on which terms dominate in the momentum equation. For scenarios that are dominated by frictional forces (i.e. the array radius is large compared to the water depth), the maximum power is a fraction of the power dissipated by friction within the boundary of the array when no turbines are present. If the flow is dominated by the advective terms of the momentum equation, the maximum power is a fraction of the kinetic energy flux through the frontal area of the array.

Vennell [154] applies the 1D model to two types of tidal flows, a shallow channel (relative to turbine diameter) that is dominated by frictional drag, and a deep channel that is dominated by the flow inertia. The results show that for the shallow channel, a blockage ratio of 0.1 can achieve an array efficiency of 0.5, but the deep channel requires a much higher blockage ratio of 0.5 to achieve a comparable array efficiency. Achieving a high blockage ratio in a deep channel requires large turbines (or a stackable design). As Vennell [154] notes however, it is important to remember that in most cases the blockage ratio will be limited by the need to maintain navigation and to limit the environmental impact of an array.

Building on the linear momentum actuator disk model of Garrett and Cummins [52], Nishino and Willden [115] developed a single row turbine array model that takes into account intra-row spacing and the portion of the channel width taken up by the partial fence of turbines. They found that (for a shallow channel) an array that occupies only a small fraction of the channel width will have an optimal intra-row spacing for maximizing the array's
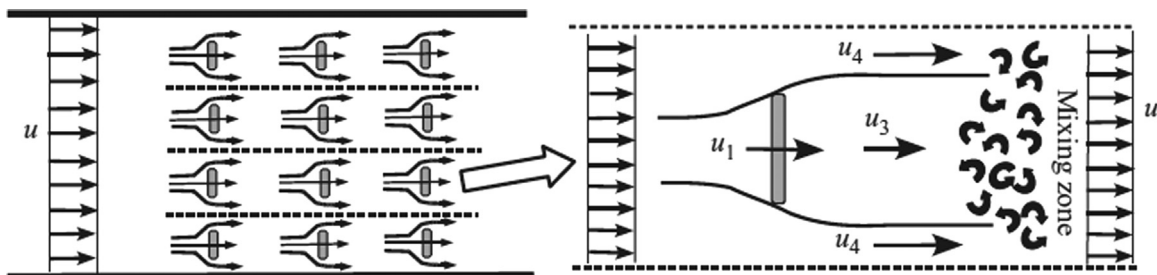

Fig. 8. Diagram of velocity definitions for a turbine in an array. Figure copied from [153].

efficiency. For an infinitely wide channel, it is shown analytically that the energy extraction efficiency of an array increases from the Betz limit of 0.593 when the local blockage is zero (i.e. when the intra-row spacing is much greater than the turbine diameter) to a limit of 0.798 when the local blockage is optimized. Beyond this optimal local blockage value (≈ 0.40) the array efficiency decreases.

A linear momentum actuator-disk-theory model has also been used to compare the effects of staggered and centered rows of turbines on array efficiency [32]. For a fixed number of turbines, two staggered rows are found to be more efficient than two centered rows, but a single row is more efficient than both arrangements. Intra-row spacing is also investigated for a laterally unconfined array. It is found that the intra-row spacing for a two-row, staggered arrangement should be much greater than that for a single row for maximum efficiency. Also, the optimal streamwise spacing between rows depends on the number of rows in an array. One advantage of staggered arrangements is that the kinetic energy between two turbines can be increased by as much as 22% due to the local flow acceleration. A third, downstream staggered turbine can take advantage of this energized flow to increase an array's efficiency [102,104].

3.4.2. Array numerical modeling (CFD)

The CFD literature is still converging on the best techniques for modeling turbine arrays. The difficulty lies in the complex, turbulent structures created by the rotating components.

The one-dimensional linear momentum models of [51,52], which represent turbines as a drag force, have been implemented numerically [60,1,162]. Free-surface effects have also been modeled theoretically [160] and numerically [33]. The most advanced numerical models consider turbine drag, free-surface effects, as well as factors such as array blockage ratio, multiple turbine rows, seasonal flow variation, bed friction variation, and the optimal tuning of individual turbines [1]. A recent study on the effects of blockage ratio and turbine design on the energy output of a tidal fence reinforce the concept that turbines must be designed for the flow conditions created by the full array [134].

Instead of a drag force, some numerical models represent turbines with a specific flow velocity reduction [161]. This method allows the velocity ratio through a turbine array to be adjusted for optimal performance in a given site.

A significant amount of CFD modeling has focused on the optimal configuration of turbines within an array. Churchfield et al. [24] modeled rows of horizontal axis turbines with a 3D large eddy simulation to show that arrays with high blockage ratios and small intra-row spacing can benefit from staggered positions. They also found a small benefit from counter-rotating adjacent turbines. Confirming this, Bai et al. [12] shows that staggered arrays are more efficient than centered arrays. They conclude that an intra-row spacing of 2.5 diameters is ideal for staggered rows. They find that a two-row staggered arrangement can achieve an 11% greater efficiency than the same amount of isolated turbines. Xue et al. [161] also finds that staggered rows are more efficient using a large numerical model of a specific tidal site.

Funke et al. [49] combines the ideas of micro-siting turbines relative to each other and tuning each turbine within an array for optimum performance in a nonlinear 2D shallow water equation solver. Their gradient-based algorithm optimizes the layout of several hundred turbines for maximum array power production.

3.4.3. Array experimental research

Due to the constraints of test facilities, there remains a dearth of experimental HEC array studies. One experimental study used three identical axial-flow turbines to investigate the effects of streamwise distance on the performance of a turbine in an array

[143]. One series of experiments considered two turbines placed coaxially at distances of five, eight, and eleven diameters; the downstream turbine was found to have faster wake recovery than its upstream counterpart. In another series of experiments, a third coaxially-placed turbine also had enhanced wake recovery, similar to the second, midstream turbine. Stelzenmuller and Aliseda [143] theorize that the turbulence in the upstream wakes (which is the inflow to the downstream turbine) enhances the downstream wake recovery. These findings reinforce the idea that ambient turbulence can enhance wake recovery [96].

Recent experimental studies for optimal placement of turbines in arrays are using more large scale models and test facilities [69]. The Marine Research Group at Queen's University Belfast has built a barge to conduct tests of 1/10 scale turbines with various configurations. So far only steady tests have been conducting in a lake but there are plans to do similar tests in more realistic flows.

Mesh disk models have also demonstrated that the wake turbulence from an upstream turbine (mesh disk) can aid in the wake recovery of a second, downstream turbine (mesh disk) [11]. It is important to remember that the amount of wake recovery achieved can depend on a multitude of factors, including the geometry of a test channel, the geometry of the turbine, and the inflow conditions. This fact makes it difficult to compare results from various studies and to extrapolate them to real world applications.

3.5. Environmental impact

Optimal array performance must be balanced with the environmental impacts of energy extraction [27,19,28,124]. Furthermore, environmental impact studies must be used to inform decision making by project stakeholders and regulating bodies throughout all phases of project development [45].

In 2012, the European Commission completed its Equimar project, which developed protocols for "equitable testing and evaluation of marine energy extraction devices in terms of performance, cost, and environmental impact" [46]. Equimar noted in its summary on environmental impact assessments that very few impact studies have been done. Since that time, a paucity of environmental impact assessments remains, primarily due to the lack of installations.

Copping et al. [26] review three areas of environmental concern:

- blade strikes with marine life;
- effects of HEC sounds on marine life;
- effects on the physical environment due to energy extraction and flow alteration.

Research to date suggests that blade strikes are a nonissue. In most cases observed, marine life avoids the turbines altogether, and in the few cases observed when fish actually pass through the turbine swept area, the survival rates have been 98% or higher [26,36,21]. Further, a detached-eddy simulation of a three-bladed axial-flow turbine, with fish modeled as *passive* Lagrangian particles, demonstrates survival rates of 96% or more [131]. *In situ* studies also indicate that larger marine life generally avoid hydrokinetic turbines [78,147]. Tomichek et al. [147] monitored the interactions between live, tagged fish and Verdant's axial-flow turbines in the East River; the fish generally avoided the faster-flowing regions of the river, where the turbines are situated.

There are numerous models for the effects on the physical environment caused by tidal turbine arrays (e.g. [3,60,148,114,162,77]). Couch and Bryden [28] were early leaders in the field; one important result their model showed was that a turbine array will not cause a significant water elevation drop, as previously feared. This result has

since been confirmed [148]. Arrays will, however, impact the velocity and turbulence of a flow, which has implications for soil and sediment transport [112,113]. One model indicates that tidal arrays could impact suspended sediment concentrations at downstream distances of up to 1.6 times the array length [3]. A more recent study indicates that first generation arrays (with capacities less than 50 MW) will not affect sediment transport beyond the limits of the natural variability found before array installation [128].

In addition to environmental impacts, sediment transport can affect the performance of an array and the integrity of anchoring structures. In inland flows, large dunes develop and change with flow patterns. Introducing turbines will alter the creation of these dunes and associated troughs in the river bed [61]. While the interference of large sediment structures is of relatively small concern today, as the cost of hydrokinetic energy comes down and the environmental impact of arrays is better understood, large river sites with their associated large sediment structures will be targeted for future development [62].

Other areas of environmental concern include [44,20,137]:

- construction spills and device leakage effects on water quality;
- the effect of electromagnetic fields on marine life;
- habitat alteration due to the introduction of artificial structures;
- array impact on marine life movement patterns; and
- benthic predators' ability to find prey.

The Tethys Database [145] acts as a repository for environmental impact information for HEC devices (and offshore wind technology).

4. Outlook

The HEC industry has many designs that have completed (or nearly completed) commercial-scale testing. The next step in industry will be the deployment of small arrays. Array installations are projected to begin in earnest in 2016–2017 (see Fig. 9). The Meygen project (in Scotland) is scheduled for construction in 2016; it will include 269 turbines and has the potential to provide up to 16.6 TWh/yr, which represents 45% of Scotland's 2011 electricity consumption [1]. Starting in 2017, GDF Suez plans to develop France's most energy dense tidal site, Raz Blanchard [54]. Tocardo of the Netherlands could also be a key player in the development of tidal arrays in the near future [146]. Tocardo and Manx Tidal Energy have been selected by the Isle of Man to develop a tidal energy project in its waters [66]. The St. Lawrence River project in Montreal could be the world's first inland hydrokinetic array [16].

The HEC industry faces several major hurdles, some in the form of policy, regulation, and socioeconomic factors. Policy and regulation can either be a barrier or boost to industry. The UK, France, Ireland, Australia, Canada, and South Korea all have policies that promote research and development of tidal technologies [79]. These countries have made clear renewable energy goals, many provide special funding programs for HEC research, and Canada and the UK provide open-sea testing centers. In other countries, including the US, lack of consistent energy policy and complicated regulation structures inhibit technology growth. VanZwieten et al. [152] present an overview of the regulatory issues affecting HEC technology in the US.

Socioeconomic and environmental impacts have been identified as the two most important factors affecting future investment in HEC technology [98]. These two issues can overlap when public concern centers around the environmental impacts of HEC devices [72]. To advance HEC technology, researchers must clearly assess the environmental impacts of HEC arrays, and developers must ensure that the public is well informed and does not fear these environmental impacts [67]. (Bonar et al. [17] provide a recent summary of these social and ecological issues.) Other important socioeconomic factors that will affect HEC technology development in the future include: stakeholder participation, including governmental, environmental, community and industry organizations; supply chain and workforce development; user conflicts; and developing lender confidence [63].

Another major barrier to HEC technology development is lack of industry cooperation [79,116]. Cooperative industry organizations can aid in advancing the technology by pooling resources to affect energy policies that provide more funding for research and to promote public education and support. In the US, the greatest step towards addressing this issue was the formation of the Ocean Renewable Energy Coalition (OREC) in 2005 [118]. Unfortunately, only a small number of HEC technology companies have joined OREC so far. Ocean Energy Europe (OEE) [117] provides a good example of effective industry cooperation. Ocean Energy Europe's membership includes numerous large and small businesses, major research centers, and other national policy groups. The OEE group works directly with the European Commission and other government institutions in developing energy policy. Magagna and Uihlein [95] provide a summary of the current status of HEC technology in Europe.

To summarize, the hydrokinetic industry is poised to install commercial-scale inland and tidal arrays in the near future. Key issues to be addressed to promote the industry include favorable government policy and regulation, socioeconomic and environmental issues, and industry cooperation.
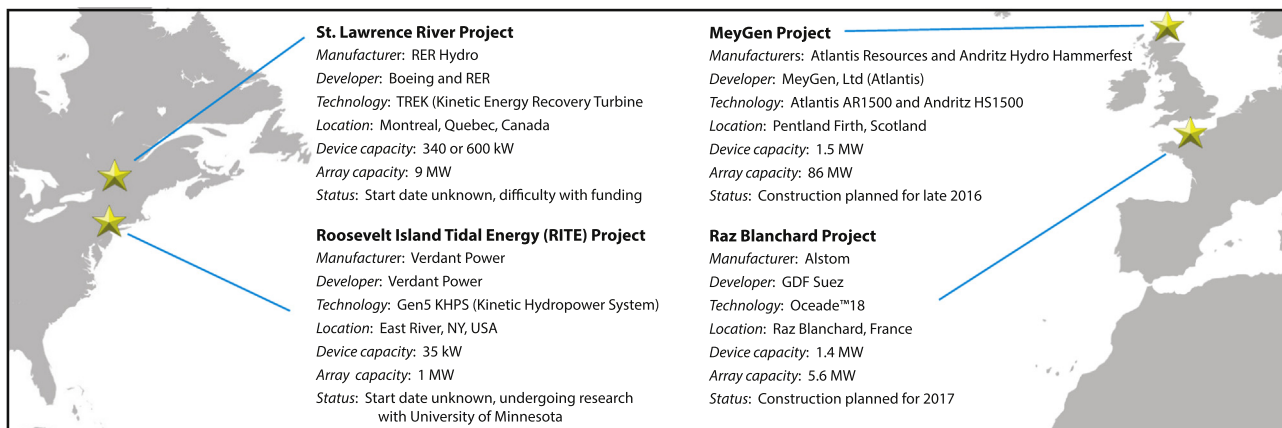

St. Lawrence River Project
Manufacturer: RER Hydro
Developer: Boeing and RER
Technology: TREK (Kinetic Energy Recovery Turbine)
Location: Montreal, Quebec, Canada
Device capacity: 340 or 600 kW
Array capacity: 9 MW
Status: Start date unknown, difficulty with funding

Roosevelt Island Tidal Energy (RITE) Project
Manufacturer: Verdant Power
Developer: Verdant Power
Technology: Gen5 KHPS (Kinetic Hydropower System)
Location: East River, NY, USA
Device capacity: 35 kW
Array capacity: 1 MW
Status: Start date unknown, undergoing research with University of Minnesota

MeyGen Project
Manufacturers: Atlantis Resources and Andritz Hydro Hammerfest
Developer: MeyGen, Ltd (Atlantis)
Technology: Atlantis AR1500 and Andritz HS1500
Location: Pentland Firth, Scotland
Device capacity: 1.5 MW
Array capacity: 86 MW
Status: Construction planned for late 2016

Raz Blanchard Project
Manufacturer: Alstom
Developer: GDF Suez
Technology: Oceade™18
Location: Raz Blanchard, France
Device capacity: 1.4 MW
Array capacity: 5.6 MW
Status: Construction planned for 2017

Fig. 9. Hydrokinetic array projects.

5. Conclusions

This paper provides a broad review of hydrokinetic energy conversion technology research and development. By doing so the key hurdles to widespread commercialization of HEC technology are identified. In short, the key hurdles are:

- reducing the cost of energy,
- optimizing individual turbines to work in concert considering array and bathymetry effects,
- balancing energy extraction with environmental impact,
- and addressing socioeconomic concerns.

There are many pathways to affect the costs of an HEC system. Two of the greatest impact areas may be (i) increasing the reliability of HEC systems and (ii) optimizing turbines for array flow conditions. Given the expensive process of retrieving systems at sea and in rivers for maintenance and service, it is vital to increase the reliability of HEC systems. This can be done by directing more research towards health monitoring and predictive maintenance systems, as well as developing more robust and simple designs. Regarding array performance, turbines must be designed for the loads and flow conditions that will occur after all turbines are installed. The research indicates that turbines optimized for solitary operation will perform poorly in an array, and individualized tuning of turbines in the array configuration is needed for optimal array performance.

Gaining more knowledge on the environmental impacts of HEC devices is crucial to expediting the permitting and licensing process of projects. In order to do this, public support must be gained. Unfortunately, most people are unaware of the advanced state of HEC technology. If they are aware of the technology, they usually fear that installations will destroy marine life and take away the livelihood of local fishermen. To help address these issues the US Department of Energy recently invested $3.25 million across five different research centers focusing on noise issues and marine life interaction with hydrokinetic devices [65]. An additional $4 million has been invested in a consortium that will work on array designs, system performance enhancements, and biological monitoring.

In summary, the areas of research reviewed and industry issues discussed in this paper reflect the topics that are crucial to advancing HEC technology. With demonstration projects currently installing turbines and researchers addressing the open questions, it is clear that hydrokinetic energy conversion technology will play an important role in renewable energy generation around the world. Installations will occur first in remote locations where energy costs are high and therefore HEC technology can compete with the existing energy infrastructure. Early installations are also possible in locations with no existing energy infrastructure and rich hydrokinetic resources. And, as the Meygen project indicates, governments with a commitment to increasing renewable energy production will lead the way in developing hydrokinetic resources.

References

[1] Thomas A, Adcock A. The available power from tidal stream turbines in the Pentland Firth. Proc R Soc; 2013.
[2] Admiralty inlet project summary (Tethys). URL ⟨http://mhk.pnnl.gov/annex-iv-sites/admiralty-inlet-pilot-tidal-project#_jmp0_⟩; 2014.
[3] Ahmadian R, Falconer R, Bockelmann-Evans B. Far-field modelling of the hydro-environmental impact of tidal stream turbines. Renew Energy; 2012.
[4] Alaska Center for Energy and Power. Alaska hydrokinetic technology development and demonstration: a project by ORPC Alaska, LLC. Technical report. University of Alaska Fairbanks; 2013.
[5] Alaska Renewable Energy. URL ⟨http://alaskarenewableenergy.org/why-renewable-energy-is-important/alaskas-resources/⟩; 2014.
[6] Arango MA. Resource assessment and feasibility study for use of hydrokinetic turbines in the tailwaters of the priest rapids project [Master's thesis]. University of Washington; 2011.
[7] Atlantis Resources. URL ⟨http://atlantisresourcesltd.com/technology.html#_jmp0_⟩; 2014.
[8] Bachant P, Wosnik M. Reynolds number dependence of cross-flow turbine performance and near-wake characteristics. In: Proceedings of the 2nd marine energy technology symposium; 2014.
[9] Bachant P, Wosnik M. Performance measurements of cylindrical- and spherical-helical cross-flow marine hydrokinetic turbines, with estimates of exergy efficiency. Renew Energy; 2015.
[10] Bahaj AS. Characterising the wake of horizontal axis marine current turbines. In: Proceedings of the 7th European wave and tidal energy conference. Porto, Portugal; 2007.
[11] Bahaj AS, Myers LE. Shaping array design of marine current energy converters through scaled experimental analysis. Energy 2013.
[12] Bai G, Li J, Fan P, Li G. Numerical investigations of the effects of different arrays on power extractions of horizontal axis tidal current turbines. Renew Energy; 2013.
[13] Batten WMJ, Harrison ME, Bahaj AS. Accuracy of the actuator disc-rans approach for predicting the performance and wake of tidal turbines. R Soc 2013.
[14] Beam MJ, Kline BL, Elbing BE, Straka W, Fontaine AA, Lawson Michael, et al. Marine hydrokinetic turbine power-take-off design for optimal performance and low impact on cost-of-energy. In: Proceedings of the ASME 2013 32nd international conference on ocean, offshore and Arctic engineering; 2013.
[15] Bernitsas MM. VIVACE (vortex induced vibration aquatic clean energy): a new concept in generation of clean and renewable energy from fluid flow. Offshore Mech Arct Eng; 2008.
[16] Boeing and RER Hydro. URL ⟨http://boeing.mediaroom.com/Boeing-and-RER-Hydro-to-Provide-Quebec-with-Clean-Hydrokinetic-Power#_jmp0_⟩; November 2013.
[17] Bonar PAJ, Bryden IG, Borthwick AGL. Social and ecological impacts of marine energy development. Renew Sustain Energy Rev 2015;47.
[18] Bruce A.J. Tidal energy system for on-shore power generation. Technical report. DOE Marine and Hydrokinetic Technology Readiness Initiative; 2012.
[19] Bryden IG, Couch SJ. Me1–marine energy extraction: tidal resource analysis. Renewable Energy 2006;31(2):133–9 [ISSN 0960-1481].
[20] Cada G, Ahlgrimm J, Bahleda M, Bigford T, Stavrakas SD, Hall D, et al. Potential impacts of hydrokinetic and wave energy conversion technologies on aquatic environments. Fisheries 2007.
[21] Castro-Santos T, Haro A. Survival and behavioral effects of exposure to a hydrokinetic turbine on juvenile Atlantic salmon and adult American shad. Estuar Coasts 2015;38.
[22] Chamorro LP, Troolin DR, Lee Seung-Jae. Three-dimensional flow visualization in the wake of a miniature axial-flow hydrokinetic turbine. Exp Fluids 2013.
[23] Chang Che-Chun. Hydrokinetic energy harnessing using the vivace converter with passive turbulence control. In: Proceedings of the ASME 2011 30th international conference on ocean, offshore and Arctic engineering; 2011.
[24] Churchfield MJ, Li Y, Moriarty PJ. A large-eddy simulation study of wake propagation and power production in an array of tidal-current turbines. In: 9th European wave and tidal energy conference; 2011.
[25] Clarke J, Connor G, Grant A, Johnstone C, Ordonez-Sanchez S. Contra-rotating marine current turbines: Single point tethered floating system—stability and performance. In: Proceedings of the 8th European wave and tidal energy conference. Uppsala, Sweden; 2009.
[26] Copping A, Battey H, Brown-Saracino J, Massaua M, Smith C. An international assessment of the environmental effects of marine energy development. Ocean Coast Manag 2014.
[27] Couch SJ, Bryden I. The impact of energy extraction on tidal flow development. In 3rd IMarEST international conference on marine renewable energy; 2004.
[28] Couch SJ, Bryden IG. Large-scale physical response of the tidal system to energy extraction and its significance for informing environmental and ecological impact assessment. In: Proceedings of the OCEANS; 2007.
[29] Daly T, Myers LE, Bahaj AS. Modelling of the flow field surrounding tidal turbine arrays for varying positions in a channel. R Soc 2013.
[30] Ding L, Bernitsas MM, Kim ES. 2-d urans vs. experiments of flow induced motions of two circular cylinders in tandem with passive turbulence control for $30,000 < Re < 105,000$. Ocean Eng; 2013.
[31] Ding L, Zhang L, Bernitsas Michael M, Chang Che-Chun. Numerical simulation and experimental validation for energy harvesting of single-cylinder vivace converter with passive turbulence control. Renew Energy 2015;85.
[32] Draper S, Nishino T. Centred and staggered arrangements of tidal turbines. J Fluid Mech 2014.
[33] Draper S, Houlsby GT, Oldfield MLG, Borthwick AGL. Modelling tidal energy extraction in a depth-averaged coastal domain modelling tidal energy extraction in a depth-averaged coastal domain modelling tidal energy extraction in a depth-averaged coastal domain. In: Proceedings of the 8th European wave and tidal energy conference; 2009.
[34] Drela M. Xfoil: an analysis and design system for low Reynolds number airfoils. In: Low Reynolds number aerodynamics: proceedings for the conference. Notre Dame, IN: Springer-Verlag; 1989.
[35] EERE marine and hydrokinetic resource assessment and characterization. URL ⟨http://energy.gov/eere/water/marine-and-hydrokinetic-resource-assessment-and-characterization⟩; 2014.

[36] Electric Power Research Institute. Environmental effects of hydrokinetic turbines on fish. Technical report. Electric Power Research Institute; 2012.

[37] Electric Power Research Institute. Assessment and mapping of the riverine hydrokinetic energy resource in the Continental United States. Technical report, Electric Power Research Institute; 2012.

[38] Epps BP, Stanway MJ, Kimball RW. Openprop: an open-source design tool for propellers and turbines. In: SNAME propellers and shafting; 2009.

[39] Epps BP, Kimball RW. OPENPROP: Open-source software for the design and analysis of marine propellers and horizontal-axis turbines. URL ⟨http://engineering.dartmouth.edu/epps/openprop⟩; 2013.

[40] Brenden E. An impulse framework for hydrodynamic force analysis: fish propulsion, water entry of spheres, and marine propellers [Ph.D. thesis]. MIT; 2010.

[41] Brenden E. CYROD: Open-source software for the design and analysis of vertical-axis propellers and turbines. URL ⟨http://engineering.dartmouth.edu/epps/cyrod⟩; 2014.

[42] Epps B, Víquez O, Chryssostomidis Chryssostomos. A method for propeller blade optimization and cavitation inception mitigation. J Ship Prod Des 2014;30(3):1–12.

[43] Epps BP, Kimball RW. Unified rotor lifting line theory. J Ship Res 2013;57 (December).

[44] EquiMar. Uncertainties regarding environmental impacts. Technical report. EquiMar; 2009.

[45] EquiMar. Assessment of the present status and future scenarios of the supply chain for marine energy arrays. Technical report. EquiMar; 2011.

[46] EquiMar. URL ⟨https://www.wiki.ed.ac.uk/display/EquiMarwiki/EquiMar⟩; 2012.

[47] European Marine Energy Centre. URL ⟨http://www.emec.org.uk/⟩; 2014.

[48] Flumill. URL ⟨http://www.flumill.com/www.flumill/The_Technology/content-1.html⟩; 2014.

[49] Funke SW, Farrelld PE, Piggott MD. Tidal turbine array optimisation using the adjoint approach. Renew Energy 2014.

[50] Galloway PW, Myers LE, Bahaj AS. Quantifying wave and yaw effects on a scale tidal stream turbine. Renew Energy 2014.

[51] Garrett C, Cummins P. The power potential of tidal currents in channels. Proc R Soc; 2005.

[52] Garrett C, Cummins P. The efficiency of a turbine in a tidal channel. J Fluid Mech 2007.

[53] Garrett C, Cummins P. Garrett maximum power from a turbine farm in shallow water. J Fluid Mech 2013.

[54] Suez GDF, Blanchard R. URL ⟨http://www.gdfsuez.com/en/journalists/press-releases/gdfsuez-signs-industrial-partnership-agreement-tidal-power-project-raz-blanchard/⟩; February 2013.

[55] Georgia Tech Research Corporation. Assessment of energy production potential from tidal streams in the United States. Technical report. Wind & Water Power Program, Office of Energy Efficiency and Renewable Energy of the U.S. Department of Energy; 2011.

[56] Georgia Tech Research Corporation. Assessment of energy production potential from ocean currents along the United States coastline. Technical report. Wind & Water Power Program, Office of Energy Efficiency and Renewable Energy of the U.S. Department of Energy; 2013.

[57] Gosselin R. Optimization of vertical-axis turbine using numerical simulations. URL ⟨http://www.lmfn.ulaval.ca/en/projets_de_recherche/ener_renouv/eolienne_a_ailes_verticales/optimisation_des_turbines_a_axes_verticales/⟩.

[58] Gunawan B, Neary Vincent S, Colby J. Tidal energy site resource assessment in the east river tidal strait, near Roosevelt Island, New York, New York. Renew Energy; 2014.

[59] Harrison ME, Batten WMJ, Myers LE, Bahaj AS. A comparison between cfd simulations and experiments for predicting the far wake of horizontal axis tidal turbines. In: Proceedings of the 8th European wave and tidal energy conference; 2009.

[60] Hasegawa D, Sheng J, Greenberg DA, Thompson KR. Far-field effects of tidal energy extraction in the Minas Passage on tidal circulation in the Bay of Fundy and Gulf of Maine using a nested-grid coastal circulation model. Ocean Dyn 2011.

[61] Hill C, Musa M, Chamorro LP, Ellis C, Guala M. Local scour around a model hydrokinetic turbine in an erodible channel. J Hydraul Eng 2014.

[62] Hill C, Musa M, Guala M. Interaction between instream axial flow hydrokinetic turbines and uni-directional flow bedforms. Renew Energy 2016;86.

[63] Howell A, Drake C. Scoping study on socio-economic impacts of tidal energy development in Nova Scotia: a research synthesis & priorities for future action. Technical report. Fundy Energy Research Network; 2012.

[64] HydroWorld.com. Siemens announces plan to exit marine power sector. URL ⟨http://www.hydroworld.com/articles/2014/11/siemens-announces-plan-to-exit-marine-power-sector.html?utm_source=feedburner&utm_medium=feed&utm_campaign=Feed%3A+HydroworldcomNews+%28HydroWorld+News%29⟩.

[65] HydroWorld.com. Doe awards 3.25 million to advance mhk technologies. URL ⟨http://www.hydroworld.com/articles/hr/print/volume-33/issue-9/departments/marine-hydrokinetics.html⟩; 2014.

[66] HydroWorld.com. Isle of man prepares for marine hydrokinetic development. URL ⟨http://www.hydroworld.com/articles/2014/11/isle-of-man-prepares-for-marine-hydrokinetic-development.html⟩; 2014.

[67] Jansujwicz Jessica S, Johnson TR. Human dimensions research on marine hydrokinetic energy development in Maine. In: Proceedings of the 2nd international conference on environmental interactions of marine renewable energy technologies; 2014.

[68] Javaherchi T, Stelzenmuller N, Seydel J, Aliseda A. Experimental and numerical analysis of a scale-model horizontal axis hydrokinetic turbine. In: Proceedings of the 2nd marine energy technology symposium; 2014.

[69] Jeffcoate P, Whittaker T, Boake C, Elsaesser B. Field tests of multiple 1/10 scale tidal turbines in steady flows. Renew Energy 2016;87.

[70] Jenne DS, Yu Y-H, Neary V. Levelized cost of energy analysis of marine and hydrokinetic reference models. In: 3rd marine energy technology symposium; 2015.

[71] Johnson J.B, Pride D.J. River, tidal, and ocean current hydrokinetic energy technologies: status and future opportunities in Alaska. Technical report. Alaska Center for Energy and Power; 2010.

[72] Johnson T, Zydlewski GB. Research for the sustainable development of tidal power in maine. Maine Policy Rev 2012;21(1) [Sustainability].

[73] Kahn MJ, Iqbal MT, Quaicoe JE. Design considerations of a straight bladed darrieus rotor for river current turbines. In: IEEE ISIE, Montreal, Quebec, CA; July 9–12, 2006.

[74] Kang S, Borazjani I, Colby JA, Sotiropoulos F. Numerical simulation of 3d flow past a real-life marine hydrokinetic turbine. Adv Water Res 2012;39.

[75] Kang S, Yang X, Sotiropoulos F. On the onset of wake meandering for an axial flow turbine in a turbulent open channel flow. J Fluid Mech 2014.

[76] Karbasian HR, Esfahani JA, Barati E. Simulation of power extraction from tidal currents by flapping foil hydrokinetic turbines in tandem formation.pdf. Renew Energy 2015;81.

[77] Kartezhnikova M, Ravens TM. Hydraulic impacts of hydrokinetic devices. Renew Energy 2014.

[78] Keenan G, Sparling C, Williams H, Fortune F. Seagen environmental monitoring programme final report. Technical report. Royal Haskoning; 2011.

[79] Kempener R, Neumann F. Tidal energy technology brief. Technical report. International Renewable Energy Agency; 2014.

[80] Kinsey T, Dumas G. Optimal operating parameters for an oscillating foil turbine at Reynolds number 500,000. AIAA J; 2014.

[81] Kinsey T, Dumas G, Lalande G, Ruel J, Méhut A, Viarouge P, et al. Prototype testing of a hydrokinetic turbine based on oscillating hydrofoils. Renew Energy 2011.

[82] Kinsey T, Dumas G. Computational fluid dynamics analysis of a hydrokinetic turbine based on oscillating hydrofoils. J Fluids Eng 2012.

[83] K. T, Dumas G. Three-dimensional effects on an oscillating-foil hydrokinetic turbine. J Fluids Eng 2012.

[84] Kinsey T, Dumas G. Optimal tandem configuration for oscillating-foils hydrokinetic turbine. J Fluids Eng 2012.

[85] Kolekar N, Banerjee A. Performance characterization and placement of a marine hydrokinetic turbine in a tidal channel under boundary proximity and blockage effects. Appl Energy 2015;148.

[86] Kolekar N, Banerjee A. A coupled hydro-structural design optimization for hydrokinetic turbines. J Renew Sustain Energy 2014.

[87] K., Cohen, Dowling. Fluid mechanics. 5th ed. Academic Press; 2012.

[88] LaBonte A, O'Connor P, Fitzpatrick C, Hallett K, Li Y. Standardized cost and performance reporting for marine and hydrokinetic technologies. In: Proceedings of the 1st marine energy technology symposium; 2013.

[89] Lago LI, Ponta FL, Chen L. Advances and trends in hydrokinetic turbine systems. Energy Sustain Dev 2010.

[90] Li Ye, Karri N, Wang Qi. Three-dimensional numerical analysis on blade response of a vertical-axis tidal current turbine under operational conditions. J Renew Sustain Energy 2014.

[91] Lust EE, Luznik Luksa, Flack Karen A, Walker Jessica M, Van Benthem Max C. The influence of surface gravity waves on marine current turbine performance. Int J Marine Energy 2013.

[92] Luznik L, Van Benthem M, Flack KA, Lust EE. Near wake characteristics of a model horizontal axis marine current turbine under steady and unsteady inflow conditions. In: OCEANS. CA: IEEE San Diego; 2013.

[93] Luznik L, Flack KA, Lust EE, Taylor K. The effect of surface waves on the performance characteristics of a model tidal turbine. Renew Energy 2013.

[94] MacLeod AJ, Barnes S, Rados KG, Bryde IG. Wake effects in tidal current turbine farms. In: Marine renewable energy conference; 2002.

[95] Magagna D, Uihlein A. Ocean energy development in Europe: current status and future perspectives. Int J Marine Energy 2015;11.

[96] Maganga F, Germain G, King J, Pinon G, Rivoalen E. Experimental characterisation of flow effects on marine current turbine behaviour and on its wake properties. IET Renew Power Gener 2010.

[97] Maisondieu C, Johanning L, Weller S. Best practice report—installation procedures. Technical report. Marine Energy in Far Peripheral and Island Communities; 2014.

[98] Marine and Hydrokinetic Energy Technology Assessment Committee. An evaluation of the U.S. Department of Energy's Marine and Hydrokinetic Resource Assessments. Technical report. National Research Council; 2013.

[99] Marine current turbines. URL ⟨http://www.marineturbines.com/About-Marine-Current-Turbines⟩; 2014.

[100] Marine current turbines projects with Siemens. URL ⟨http://www.marineturbines.com/Projects⟩; 2014.

[101] Michelen C, Neary VS, Murray JC, Barone M. Cactus open source code for hydrokinetic turbine design and analysis: model performance evaluation and public dissemination as open source design tool. In: Proceedings of the 2nd marine energy technology symposium; 2014.

[102] Myers LE, Keogh B, Bahaj AS. Experimental investigation of inter-array wake properties in early tidal turbine arrays. In: OCEANS; 2011.

[103] Myers LE, Bahaj AS. Experimental analysis of the flow field around horizontal axis tidal turbines by use of scale mesh disk rotor simulators. Ocean Eng; 2010.

[104] Myers LE, Bahaj AS. An experimental investigation simulating flow effects in first generation marine current energy converter arrays. Renew Energy 2012;37(1):28–36. http://dx.doi.org/10.1016/j.renene.2011.03.043 [ISSN 0960-1481. URL ⟨http://www.sciencedirect.com/science/article/pii/S0960148111001716⟩].

[105] Myers LE, Bahaj AS, Rawlinson-Smith RI, Thomson M. The effect of boundary proximity upon the wake structure of horizontal axis marine current turbines. In: 27th international conference on offshore mechanics and Arctic engineering; 2008.

[106] Myers L, Bahaj AS, Gregory G, Jack G. Flow boundary interaction effects for marine current energy conversion devices. In: 10th world renewable energy congress; 2008.

[107] Nautricity (Cormat). URL ⟨http://www.nautricity.com/cormat/⟩; 2014.

[108] Neary VS, Gunawan B, Richmond MC, Durgesh V, Polagye B, Thomson J, et al. Field measurements at river and tidal current sites for hydrokinetic energy development: best practices manual. Technical report. Oak Ridge National Laboratory; 2011.

[109] Neary VS, Gunawan B, Hill C, Chamorro LP. Near and far field flow disturbances induced by model hydrokinetic turbine: ADV and ADP comparison. Renew Energy, 2013.

[110] Neary VS, Lawson M, Previsic M, Copping A, Hallett KC, LaBonte A. Methodology for design and economic analysis of marine energy conversion (MEC) technologies. In: Proceedings of the 2nd marine energy technology symposium; 2014.

[111] Nedyalkov I, Wosnik M. Cavitation investigation of hydrofoils for marine hydrokinetic turbines. Proceedings of the ASME 2013 fluids engineering division summer meeting; 2013.

[112] Neill SP, Litt EJ, Couch SJ, Davies AG. The impact of tidal stream turbines on large-scale sediment dynamics. Renew Energy, 2009.

[113] Neill SP, Jordan JR, Couch SJ. Impact of tidal energy converter (TEC) arrays on the dynamics of headland sand banks. Renew Energy 2012;37(1):387–97. http://dx.doi.org/10.1016/j.renene.2011.07.003 [ISSN 0960-1481].

[114] Ng Kai-Wern, Lam Wei-Haur, Ng Khai-Ching. 2002–2012: 10 years of research progress in horizontal-axis marine current turbines. Energies 2013;6.

[115] Nishino T, Willden RHJ. The efficiency of an array of tidal turbines partially blocking a wide channel. J Fluid Mech; 2012.

[116] NREL. Marine and hydrokinetic technology (MHK) instrumentation measurement and computer modeling workshop. Technical report. NREL; 2013.

[117] Ocean Energy Europe. URL ⟨http://www.oceanenergy-europe.eu/index.php/en/association/about-the-association⟩; 2014.

[118] Ocean Renewable Energy Coalition (About). URL ⟨http://www.oceanrenewable.com/about-orec/⟩; 2014.

[119] Ocean Renewable Power Company (Rivgen). URL ⟨http://www.orpc.co/orpcpowersystem_rivgenpowersystem.aspx⟩; 2014.

[120] OpenHydro projects. URL ⟨http://www.openhydro.com/projects.html⟩; 2014.

[121] Peterson M, Zydlewski G, Xue H, Johnson T, Cameron M, deBree G, et al. Maine tidal power initiative: environmental impact protocols for title power. Technical report. University of Maine for US Department of Energy; 2014.

[122] Plagge AM, Jestings L, Epps BP. Next-generation hydrokinetic power take-off via a novel variable-stroke hydraulic system. In: Proceedings of the ASME 2014 33rd international conference on ocean, offshore and Arctic engineering; 2014.

[123] Polagye B, Thomson J. Tidal energy resource characterization: methodology and field study in admiralty inlet, puget sound, WA, USA. J Power Energy; 2013.

[124] Polagye BL. Hydrodynamic effects of kinetic power extraction by in-stream tidal turbines [Ph.D. thesis]. University of Washington; 2009.

[125] Raghavan K, Bernitsas MM. Experimental investigation of Reynolds number effect on vortex induced vibration of rigid circular cylinder on elastic supports. Ocean Eng; 2011.

[126] RER Hydro. URL ⟨http://www.rerhydro.com/turbines/trek/⟩; 2014.

[127] Richmond M, Harding S, Romero-Gomez P. Numerical performance analysis of acoustic doppler velocity profilers in the wake of an axial-flow marine hydrokinetic turbine. Int J Marine Energy 2015;11.

[128] Robins PE, Neill SP, Lewis MJ. Impact of tidal-stream arrays in relation to the natural variability of sedimentary processes. Renew Energy, 2014.

[129] Roesler B., Francisquez M., Epps B. Design and analysis of trochoidal propulsors using nonlinear programming optimization techniques. In: 33rd international conference on ocean, offshore, and Arctic engineering (OMAE); 2014.

[130] Roesler BT, Kawamura ML, Miller E, Wilson M, Brink-Roby J, Clemmenson Eric, et al. Experimental performance of a novel trochoidal propeller. J Ship Res; 2015, in preparation.

[131] Romero-Gomez P, Richmond MC. Simulating blade-strike on fish passing through marine hydrokinetic turbines. Renew Energy, 2014.

[132] Sale D. HARP_Opt code v2.00.00. URL ⟨https://nwtc.nrel.gov/HARP_Opt⟩; June 28, 2010.

[133] Sale D, Aliseda A, Motley M, Li Y. Structural optimization of composite blades for wind and hydrokinetic turbines. In: Proceedings of the 1st marine energy technology symposium; 2013.

[134] Schluntz J, Willden RHJ. The effect of blockage on tidal turbine rotor design and performance. Renew Energy 2015;81.

[135] Schuster M, Fritz N, McEntee J, Graver T, Rumsey M, Hernandez-Sanchez B et al. Externally bonded fbg strain sensors for structural health monitoring of marine hydrokinetic structures. In: Proceedings of the 2nd marine energy technology symposium; 2014.

[136] ScotRenewables. URL ⟨http://www.scotrenewables.com/⟩; 2014.

[137] Shields MA, Woolf DK, Grist EPM, Kerr SA, Jackson AC, Harris RE, et al. Marine renewable energy: the ecological implications of altering the hydrodynamics of the marine environment. Ocean Coast Manag 2011;54(1):2–9. http://dx.doi.org/10.1016/j.ocecoaman.2010.10.036 [ISSN 0964-5691. URL ⟨http://www.sciencedirect.com/science/article/pii/S0964569110001924⟩].

[138] Shiu H, "Case" van Dam CP, Johnson E, Barone M, Phillips R, Straka W, et al. A design of a hydrofoil family for current-driven marine-hydrokinetic turbines. In ASME 2012 power conference; 2012.

[139] Sinclair B. 16.4 m turbine still in dock. URL ⟨http://www.westerntelegraph.co.uk/news/11748032.__16_4m_turbine_still_in_dock/⟩; January 25, 2015.

[140] Stallard T, Dhedin J-F, Saviot S, Noguera C. Procedures for estimating site accessibility and appraisal of implications of site accessibility. Technical report. Commission of the European Communities, EquiMar project; 2010.

[141] Stallard T, Collings R, Feng T, Whelan JI. Interactions between tidal turbine wakes: experimental study of a group of 3-bladed rotors. In: Proceedings of the 9th European wave and tidal energy conference; 2011.

[142] Stallard T, Collings R, Feng T, Whelan J. Interaction between tidal and turbine wakes: experimental study of a group of three-bladed rotors. R Soc; 2013.

[143] Stelzenmuller N, Aliseda A. Marine hydrokinetic array performance and wake characterization. Technical report. DOE EERE—Wind and Water Power Program; 2014.

[144] Tedds SC, Owen I, Poole RJ. Near-wake characteristics of a model horizontal axis tidal stream turbine. Renew Energy, 2014.

[145] Tethys database. URL ⟨http://mhk.pnl.gov⟩; 2014.

[146] The maritime executive. "What is holding tidal energy back?" URL ⟨http://www.maritime-executive.com/article/What-is-Holding-Tidal-Energy-Back-2014-09-24⟩; September 2014.

[147] Tomichek C, Colby J, Ann AM, Frisk M, Dunton K, Fox D, et al. Tagged species detection: approach to monitoring marine species at marine hydrokinetic projects. In: Proceedings of the 2nd marine energy technology symposium; 2014.

[148] Ulmgren MN. Impacts of marine hydrokinetic devices on hydrodynamics and sediment transport at fire island and east forelands in cook inlet, Alaska [Master's thesis]. University of Alaska Anchorage; 2014.

[149] University of Strathclyde. Stingray flapping wing tidal generator. URL ⟨http://www.esru.strath.ac.uk/EandE/Web_sites/05-06/marine_renewables/technology/oschydro.htm⟩.

[150] US Energy Information Administration, Electricity Consumption. URL ⟨http://www.eia.gov/forecasts/steo/report/electricity.cfm⟩; 2014.

[151] Valentine W, von Ellenrieder KD. Model scaling of ocean hydrokinetic renewable energy systems. IEEE J Ocean Eng; 2014.

[152] VanZwieten J, McAnally W, Ahmad J, Davis T, Martin J, Bevelhimer M, et al. In-stream hydrokinetic power: review and appraisal. J Energy Eng; 2014.

[153] Vennell R. Tuning turbines in a tidal channel. J Fluid Mech 2010;663:253–67. http://dx.doi.org/10.1017/S0022112010003502.

[154] Vennell R. Realizing the potential of tidal currents and the efficiency of turbine farms in a channel. Renew Energy; 2012.

[155] Vennell R. The energetics of large tidal turbine arrays. Renew Energy; 2012.

[156] Vennell R. Exceeding the betz limit with tidal turbines. Renew Energy; 2013.

[157] Vennell R, Funke Simon W, Draper Scott, Stevens Craig, Divett Tim. Designing large arrays of tidal turbines: a synthesis and review. Renew Sustain Energy Rev; 2015.

[158] Verdant Power. URL ⟨http://www.verdantpower.com⟩; 2014.

[159] Walker Jessica M, Flack Karen A, Lust Ethan E, Schultz Michael P, Luznik Luksa. Experimental and numerical studies of blade roughness and fouling on marine current turbine performance. Renew Energy; 2014.

[160] Whelan JI, Graham JMR, Piero J. A free-surface and blockage correction for tidal turbines. J Fluid Mech; 2009.

[161] Xue H, Bao M, Bao X. A numerical study of tidal farm efficiency in the western passage, US and Canada. IEEE; 2013.

[162] Yang Z, Wang T, Copping Andrea E. Modeling tidal stream energy extraction and its effects on transport processes in a tidal channel and bay system using a three-dimensional coastal ocean model. Renew Energy; 2012.

[163] Yavuz T, Koç E, Käślkäśs B, Erol O, Balas C, Aydemir T. Performance analysis of the airfoil-slat arrangements for hydro and wind turbine applications. Renew Energy; 2015.